

## Video Article

# A Neonatal Mouse Spinal Cord Compression Injury Model

Mark Züchner<sup>1,2</sup>, Joel C. Glover<sup>2,3</sup>, Jean-Luc Boulland<sup>2,3</sup><sup>1</sup>Department of Neurosurgery, Oslo University Hospital<sup>2</sup>Norwegian Center for Stem Cell Research, Oslo University Hospital<sup>3</sup>Laboratory of Neural Development and Optical Recording (NDEVOR), Department of Physiology, Institute of Basic Medical Sciences, University of OsloCorrespondence to: Jean-Luc Boulland at [jeanlb@medisin.uio.no](mailto:jeanlb@medisin.uio.no)URL: <https://www.jove.com/video/53498>DOI: [doi:10.3791/53498](https://doi.org/10.3791/53498)

Keywords: Medicine, Issue 109, neuroscience, spinal cord injury, neonatal mouse, surgery, clip, compression, plasticity

Date Published: 3/27/2016

Citation: Züchner, M., Glover, J.C., Boulland, J.L. A Neonatal Mouse Spinal Cord Compression Injury Model. *J. Vis. Exp.* (109), e53498, doi:10.3791/53498 (2016).

## Abstract

Spinal cord injury (SCI) typically causes devastating neurological deficits, particularly through damage to fibers descending from the brain to the spinal cord. A major current area of research is focused on the mechanisms of adaptive plasticity that underlie spontaneous or induced functional recovery following SCI. Spontaneous functional recovery is reported to be greater early in life, raising interesting questions about how adaptive plasticity changes as the spinal cord develops. To facilitate investigation of this dynamic, we have developed a SCI model in the neonatal mouse. The model has relevance for pediatric SCI, which is too little studied. Because neural plasticity in the adult involves some of the same mechanisms as neural plasticity in early life<sup>1</sup>, this model may potentially have some relevance also for adult SCI. Here we describe the entire procedure for generating a reproducible spinal cord compression (SCC) injury in the neonatal mouse as early as postnatal (P) day 1. SCC is achieved by performing a laminectomy at a given spinal level (here described at thoracic levels 9-11) and then using a modified Yasargil aneurysm mini-clip to rapidly compress and decompress the spinal cord. As previously described, the injured neonatal mice can be tested for behavioral deficits or sacrificed for *ex vivo* physiological analysis of synaptic connectivity using electrophysiological and high-throughput optical recording techniques<sup>1</sup>. Earlier and ongoing studies using behavioral and physiological assessment have demonstrated a dramatic, acute impairment of hindlimb motility followed by a complete functional recovery within 2 weeks, and the first evidence of changes in functional circuitry at the level of identified descending synaptic connections<sup>1</sup>.

## Video Link

The video component of this article can be found at <https://www.jove.com/video/53498/>

## Introduction

During the last decade, increasing evidence obtained from different spinal cord injury (SCI) models has shown that spinal networks can reorganize spontaneously to contribute to functional recovery<sup>1-9</sup>. Adaptive plasticity has as a consequence become an important topic in SCI research. It has been shown that plasticity encompasses regrowth of spared axons, sprouting of new axon collaterals and the formation of novel synaptic connections. Much of this knowledge has been obtained from behavioral or anatomical studies in adult animals. An important limitation of adult spinal cord studies is the difficulty of performing high-throughput physiological assessment, which is easier in neonatal preparations<sup>1</sup>. One major difference is that wholmount *ex vivo* preparations of the adult brainstem and spinal cord have low viability. Another is that adult spinal tissue is more opaque to light because it is thicker and myelinated. Although recent advances in *in vivo* imaging (see for example, <sup>10-12</sup>) may partially overcome these problems, the possibility of performing high throughput imaging at any desired dorsoventral depth at multiple sites along a given brainstem-spinal cord preparation is currently only feasible in neonates. The immature state of axon myelination in the neonatal spinal cord facilitates high-throughput *ex vivo* optical recording, thus permitting a dynamic assessment of functional synaptic connections<sup>13-17</sup>. Combined with genetically encoded calcium reporters and optogenetic stimulation and pharmacology tools, optical approaches can contribute to a deeper understanding of the mechanisms underlying adaptive plasticity.

It is estimated that between 1-10% of all spinal cord injuries affect infants and children<sup>18-22</sup>. In contrast to adult SCI the pathogenesis and potential for spontaneous recovery in pediatric SCI is less studied. Using a neonatal SCI model can therefore provide more insight into pediatric SCI and contribute to a better understanding of the pathogenetic and recovery mechanisms involved. Moreover, post-SCI plasticity supporting functional recovery in the adult spinal cord is believed to involve at least in part the same mechanisms that govern the development of the central nervous system such as axon growth, branching and formation of new synapses<sup>23-26</sup>. Thus, using a neonatal SCI model could provide important insights into mechanisms that are also operative in the adult spinal cord, or that could potentially be reinstated in the adult spinal cord (for example by implantation of fetal cells or tissue or of tissue constructed *de novo* from pluripotent stem cells) to facilitate recovery.

The neonatal mouse thus provides a platform for an integrative, multi-methodological approach to investigating adaptive plasticity following spinal cord injury, in which a combination of behavioral, physiological, anatomical, molecular and genetic methods can be readily employed. Establishing standardized neonatal injury models is an important step in implementing such studies.

## Protocol

This experimental protocol has been approved by the National Animal Research Authority in Norway (*Forsøksdyrutvalget*, local experimental approval number 12.4591) in compliance with European Union animal care regulations (Federation European Laboratory Animal Science Association). Efforts were made to minimize the number of animals used and their suffering. In this article the procedure used on postnatal (P) day 1 wild-type ICR (Imprinting Control Region) mice (Jackson, USA) is described but the same approach can also be used at later stages.

### 1. Constructing a Gas Anesthesia System for Neonatal Mice (Figure 1)

1. Build a nose-mask from the tip of a syringe. Connect this to the 3-way stopcock with plastic tubing (Figure 1 - red tubing and Figure 2A1).
2. Drill a small hole in the side of the nose mask and connect this to plastic tubing to remove the overflow of gas from the mask. End the tubing either at a vacuum pump set for a slight negative pressure, or in a fume hood (Figure 1 - bright green tubing).
3. Make an anesthesia chamber from a 150 mm x 25 mm plastic Petri dish (Figure 2A2).
  1. On one side, make a hole large enough to accommodate the head of the mouse and the nose mask.
  2. On the opposite side, make two smaller holes through which the plastic tubes to and from the nose mask can be inserted (Figure 1 - red and bright green tubing, respectively).
  3. Make a third hole on the top of the lid and attach to this a third plastic tube that ends at the vacuum pump (Figure 1 - dark green tubing). The purpose of this third tube is to ensure that any excess gas that has not been captured by the outlet from the nose mask is removed.
4. Build a sleep chamber by making a hole in the bottom of any kind of lab dish that is large enough to contain the mouse and has a smooth and even edge (the opening of the dish must lie flush with the table to prevent leakage of gas). Connect the hole in the chamber to the 3-way stopcock with plastic tubing (Figure 1 - brown tubing). Place the sleep chamber under a fume hood.
5. Connect a 3-way stopcock to the outlet tube from the vaporizer (Figure 1 - yellow tubing and Figure 2A3).
6. Connect the inlet of the vaporizer to the oxygen supply (Figure 1 - blue tubing).

### 2. Modification of a Yasargil Temporary Aneurysm Mini-clip to Create the Compression Tool (Figure 2 and Table 1)

1. Affix the clip firmly to a stand with a clamp. Using a binocular loupe for visual control, file down the outer surface of the tip of each clip blade to a final thickness of about 150  $\mu\text{m}$  using a sharpening stone mounted on a drill (Figure 2B and C).
2. Make a stopper for the clip by cutting a short stretch of polyethylene capillary tubing (Table 1) under a stereomicroscope using a micro-knife (Table 1), and place this on one of the blades (Figure 2A4 and Figures 2B and C). This prevents full closure of the clip and creates standardized compression dimensions. When the clip is closed the interblade distance is about 230  $\mu\text{m}$ . Make a new stopper for each experiment as the polyethylene material may compress during use, which would alter the interblade space.  
Note: The spring tension of the clip diminishes over time such that after about 80 compressions the clip no longer closes fully to the stopper and needs to be replaced.

### 3. Preparation Prior to Surgery

1. Place the mouse in the sleep chamber (Figure 1) and initiate anesthesia with 4% isoflurane (Figure 2A5) vaporized in pure oxygen, using a vaporizer (Figure 2A3 and Table 1).
2. Test the withdrawal reflex of the mouse by gently pinching the web of skin between the toes with a thin plastic forceps. Do this carefully as new-born mice are easily injured. Pinching too hard results in immediate bruising. Performing this test at the beginning of the sedation triggers the reflex and provides a good indication of the amount of force necessary.
3. Once the reflex is abolished, remove the mouse from the sleep chamber and place it in a prone position on the operating table with the snout inserted into the nose mask that provides a continuous supply of 4% isoflurane mixed in pure oxygen (Figure 1). Ensure that the warming pad is switched on and set to 37-38  $^{\circ}\text{C}$  as hypothermia during surgery can be fatal.
4. To achieve complete analgesia, inject subcutaneously 50  $\mu\text{l}$  of the local anesthetic Bupivacain (2.5 mg/ml, Figure 2A6) at the surgery site (in the experiments reported here, this is at thoracic level (T)9-T11). Use an insulin syringe (300  $\mu\text{l}$ , 30 G, Figure 2A7 and Table 1) to perform the injection.
5. Reduce the isoflurane concentration delivered to the nose mask to 1-2%.

### 4. Dorsal Laminectomy

1. Perform surgery under microscopic control.
2. After cleaning the surgery area with chlorhexidine gluconate (Table 1 #19) for at least 30 sec, make a 1-2 mm transverse skin incision at T9-T11 using a microknife (Figure 2A8).  
Note: In ICR neonatal mice the rostral part of the stomach, visible when it contains milk, is facing the vertebral levels T12-T13 (Figure 3). Another landmark is the rostral part of the thoracic subcutaneous adipose tissue aggregate which ends at about T8-9. This landmark is only visible after skin incision.
3. Use forceps (Figure 2A9 and A10) to widen the skin opening in a transverse direction to 8-9 mm by pulling the skin gently rostrally and caudally (the skin tears easily, creating a smooth and straight wound). This provides sufficient lateral access to the spinal column.

- Retract the edges of the skin incision from underlying structures by inserting sterile pieces of hemostatic gelatin sponge (**Figure 2A11** and **Table 1**) subcutaneously rostral and caudal to the incision. This enlarges the opening and prevents the skin from retracting and obscuring the area during surgery. The hemostatic gelatin sponge does not need to be soaked in saline prior to use.
- To expose the spine, dissect the paravertebral muscles using thin scissors (**Figure 2A12**, and **Table 1**). Cut the attachments of the muscles to the vertebral column and expose the lamina (**Figure 4A**). Note also that at this stage the spinal process is underdeveloped.
- Identify the midline and cut transversely between the two laminae (which at this stage is cartilaginous) with thin scissors (**Figure 4B**). Carefully place one blade of a thin forceps between the lamina and the dura (**Figure 4C**), grasp the lamina with the forceps and lift it carefully up until a piece breaks away, leaving the dura intact (**Figure 4D**). Repeat this 2-3 times to obtain a 1-2 segment long laminectomy.
- Using the thin forceps as rongeurs, remove parts of the facet joints bilaterally to gain enough space to place the clip within the vertebral canal. Clean the surgical area and control bleeding with small pieces of hemostatic gelatin sponge.

## 5. Spinal Cord Compression Injury

- Open the modified aneurysm mini-clip in the clip holder (**Figure 2A13** and **Figure 2B**) and place the blades on either side of the spinal cord in the spaces between the facet joints and the cord. Make sure that the blades are inserted deeply enough to affect the ventral part of the spinal cord. If this is not possible, remove more of the facet joints.
- Release the mini-clip rapidly, holding it in place with the clip holder to prevent it from sliding. Maintain the compression for 15 sec.
- Open the mini-clip rapidly and remove it. To achieve a symmetrical compression, reverse the orientation of the mini-clip, and using the easily seen mark made by the haemorrhagic edema from the first compression as a guide, reposition the clip in the reverse orientation for a second 15-sec compression (prior experiment showed that this generates symmetrical histological and physiological deficits, whereas single compressions do not<sup>1</sup>). The dura should not be damaged by the compression.
- Clean the area and maintain hemostasis with pieces of hemostatic gelatin sponge.
- Remove the pieces of hemostatic gelatin sponge that were placed under the edges of the skin incision at the start of the surgery and close the skin incision with sterile 6.0 suture and a needle holder (**Figure 2A14** and **15**).
- Inject subcutaneously 0.75 mg/kg body weight Buprenorphine (**Figure 2A16**) diluted in sterile PBS using an insulin syringe (300  $\mu$ l, 30 G).

## 6. Postoperative Care

- Remove the mouse from the nose mask and place it in a temperature-controlled chamber set at 30 °C until the anesthesia wears off and the mouse becomes alert (1-3 hr is typically sufficient).
- Inject Diazepam (**Figure 2B17**) intraperitoneally into the mother (8 g/kg body weight). This creates a torpor that diminishes the risk of cannibalism during the first night, when this risk is highest.
- Return the operated mouse to the litter.
- If the litter is large (>12 pups), remove some of the unoperated pups, preferentially the larger animals if they differ in size, to reduce competition for the milk. Maternal care of the operated pups is best in the ICR line if the litter size is around 9 pups.
- For pain management, administer Buprenorphine (0.75 mg/kg body weight) subcutaneously once a day during the first postoperative days, using an insulin syringe (300  $\mu$ l, 30 G). An appropriate volume for subcutaneous injection is 30-50  $\mu$ l. In neonatal mice vocalization and agitation are good indicators of pain.
- Perform a daily examination of the injured mice using a score sheet to evaluate nutrition, body weight, dehydration, pain, wound healing, urine retention and infection status. According to the score obtained, provide special care, such as injections of a sterile pediatric nutrition solution (**Table 1 #18**) in case of abnormal nutrition. The score sheet also defines humane endpoint criteria. A mother that does not reject the injured pups is the best caregiver.
- In the unusual case of bladder dysfunction, perform bladder massage twice a day until function is restored. This is done by placing the mouse in a supine position in one hand and massaging the lower abdomen gently in a rostro-caudal direction using a fingertip.

## Representative Results

### *Spinal cord compression injury and loss of function*

As described previously, by optimizing the preoperative, surgical and postoperative procedures, a reproducible compression SCI model in the neonatal mouse can be obtained<sup>1</sup>. The polyethylene stopper placed on one blade of the clip (**Figure 2B** and **C**) prevents the full closure of the clip and keeps the inter-blade distance consistently at about 230  $\mu$ m. Reversing the orientation of the clip in between the two compressions results in a symmetrical injury, as judged by histological sequelae (**Figure 5A** and <sup>1</sup>). Immediately after mini-clip removal, the compressed spinal cord tissue becomes darker due to hemorrhagic contusion and edema. Observation of serial sections of the injured spinal cord stained for Eosin and Hematoxylin already one day after injury reveals gradual deterioration of the tissue when approaching the lesion epicenter (**Figure 5A**). The presence of intraspinal cavities or blood in the lesion is not unusual.

Behavioral assessment, for example by tracking hindlimb trajectories under non-weight bearing conditions a few hours after surgery, shows a dramatic impairment of hindlimb motility in SCC injured mice compared to sham control mice in which only a laminectomy is performed (**Figure 5B** and <sup>1</sup>). This test can be repeated until the mouse is able to perform other behavioral tests that require bearing its own weight<sup>1</sup>.

### *Mortality and recovery after surgery*

Intraoperative mortality is mainly due to apnea and cardiac arrest caused by the high concentration of isoflurane needed to achieve sufficient anesthesia. Introducing the local anesthetic Bupivacaine into the surgical protocol permits reduction of the isoflurane concentration and thereby diminishes significantly the mortality rate. In a recent experimental series including more than 20 animals, the intraoperative mortality was nil. In contrast, post-operative survival is mainly influenced by the acceptance of the operated mice by their mother. A significant improvement occurred when anxiety and aggressiveness was reduced by delivering a single injection of Diazepam (i.p. 8 g/kg body weight) to the mother

before returning the operated mice to the litter<sup>1</sup>. Acceptance and postoperative recovery of the operated mice can be monitored by the presence of milk in the stomach. The stomach of a P1-P7 mouse that has drunken milk is clearly white and visible through the abdominal skin (**Figure 3**). Comparison of feeding in operated, sham control and unoperated mice is useful for assessing the nutritional status of injured mice. Assessing the growth of operated versus unoperated mice shows that despite a little weight loss during the first post-operative day, the growth curve of operated mice normalizes rapidly thereafter (**Figure 6**). Mortality related to bladder dysfunction or infection was never observed even in mice studied for as long as 7 weeks.

Number in Fig. 2	Name	Manufacturer/ Provider	Reference #	Link	Comment
1	Plastic syringe (30 or 50 ml)				
2	Plastic Petri dish (150 x 25 mm)				
3	Fortec isoflurane vaporizer	Cyprane		<a href="http://www.mssmedical.co.uk/products/new-vaporisers/">http://www.mssmedical.co.uk/products/new-vaporisers/</a>	We use and old device out of production, check the link for newer device
4a	Yasargil temporary aneurysm mini-clip	Aesculap	FE681K	<a href="http://www.aesculapusa.com/assets/base/doc/DOC697_Rev_C-Yasargil_Aneurysm_Clip.pdf">http://www.aesculapusa.com/assets/base/doc/DOC697_Rev_C-Yasargil_Aneurysm_Clip.pdf</a>	
4b	Fine bore polyethylene capillary tubing ID 0.58 mm, OD 0.96 mm	Smiths Medical	800/100/200	<a href="http://www.smiths-medical.com/industrialproducts/8/39/">http://www.smiths-medical.com/industrialproducts/8/39/</a>	
5	Isoflurane (Forene)	Abbott GmbH & Co. KG		<a href="http://www.life-sciences-europe.com/product/forene-abbott-gmbh-wiesbaden-group-narcotic-germany-west-2001-1858.html">http://www.life-sciences-europe.com/product/forene-abbott-gmbh-wiesbaden-group-narcotic-germany-west-2001-1858.html</a>	
6	Marcaïn (Bupivacain)	AstraZeneca		<a href="http://www.astrazeneca.co.uk/medicines01/neuroscience/Product/marcaine">http://www.astrazeneca.co.uk/medicines01/neuroscience/Product/marcaine</a>	
7	Insuline syringe 0.3 ml 30 G x 8mm	VWR	80086-442	<a href="https://us.vwr.com/store/catalog/product.jsp?product_id=4646138">https://us.vwr.com/store/catalog/product.jsp?product_id=4646138</a>	
8	Ultra Fine Micro Knife 5 mm cutting edge	Fine Science Tools	10315-12	<a href="http://www.finescience.de/katalog_ansicht.asp?Suchtyp=Kat&amp;suchkatalog=0019900000&amp;reloadmenu=1">http://www.finescience.de/katalog_ansicht.asp?Suchtyp=Kat&amp;suchkatalog=0019900000&amp;reloadmenu=1</a>	
9	Extra Fine Graefe Forceps — 0.5 mm Tip	Fine Science Tools	1153-10	<a href="http://www.finescience.de/katalog_ansicht.asp?Suchtyp=Kat&amp;suchkatalog=0055700000&amp;reloadmenu=1">http://www.finescience.de/katalog_ansicht.asp?Suchtyp=Kat&amp;suchkatalog=0055700000&amp;reloadmenu=1</a>	Not really necessary, often the teeth are too large
10	Forceps SuperGrip Straight	Fine Science Tools	00632-11	<a href="http://www.finescience.de/katalog_ansicht.asp?Suchtyp=Kat&amp;suchkatalog=0053500000&amp;reloadmenu=1">http://www.finescience.de/katalog_ansicht.asp?Suchtyp=Kat&amp;suchkatalog=0053500000&amp;reloadmenu=1</a>	Two forceps are necessary
11	Spongostan Special 70 x 50 x 1 mm	Ferrosan			
12	Vannas Spring Scissors — 2 mm Blades Straight	Fine Science Tools	15000-03	<a href="http://www.finescience.de/katalog_ansicht.asp?Suchtyp=Kat&amp;suchkatalog=0012800000&amp;reloadmenu=1">http://www.finescience.de/katalog_ansicht.asp?Suchtyp=Kat&amp;suchkatalog=0012800000&amp;reloadmenu=1</a>	
13	Vario Clip Applying Forceps	Aesculap	FE502T	<a href="http://www.aesculapusa.com/assets/base/doc/DOC697_Rev_C-Yasargil_Aneurysm_Clip.pdf">http://www.aesculapusa.com/assets/base/doc/DOC697_Rev_C-Yasargil_Aneurysm_Clip.pdf</a>	
14	Vicryl 6–0 (Ethicon)	Johnson and Johnson	J105G		
15	Diethrich micro needle holder		11-510-20	<a href="http://trimed-ltd.com/Products/Suture-Instruments/Micro-Needle-Holders-With-Tungsten-Carbide-Inserts/Ref-11-29.html">http://trimed-ltd.com/Products/Suture-Instruments/Micro-Needle-Holders-With-Tungsten-Carbide-Inserts/Ref-11-29.html</a>	

16	Temgesic (buprenorphine)	Schering-Plough		
17	Stesolid (diazepam)	Actavis		Also known as Valium
18	Pedamix	Fresenius Kabi		<a href="http://www.helsebiblioteket.no/retningslinjer/pediatri/mage-tarm-lever-ern%C3%A6ring/parenteral-ern%C3%A6ring">http://www.helsebiblioteket.no/retningslinjer/pediatri/mage-tarm-lever-ern%C3%A6ring/parenteral-ern%C3%A6ring</a>
19	Klorhexidinsprit (chlorhexidine gluconate)	Fresenius Kabi	D08A C02	<a href="http://www.felleskatalogen.no/medisin/klorhexidinsprit-fresenius-kabi-klorhexidinsprit-farget-fresenius-kabi-fresenius-kabi-560639">http://www.felleskatalogen.no/medisin/klorhexidinsprit-fresenius-kabi-klorhexidinsprit-farget-fresenius-kabi-fresenius-kabi-560639</a>

**Table 1.** List of tools and equipment for generating a clip-driven spinal cord compression injury in a neonatal mouse.

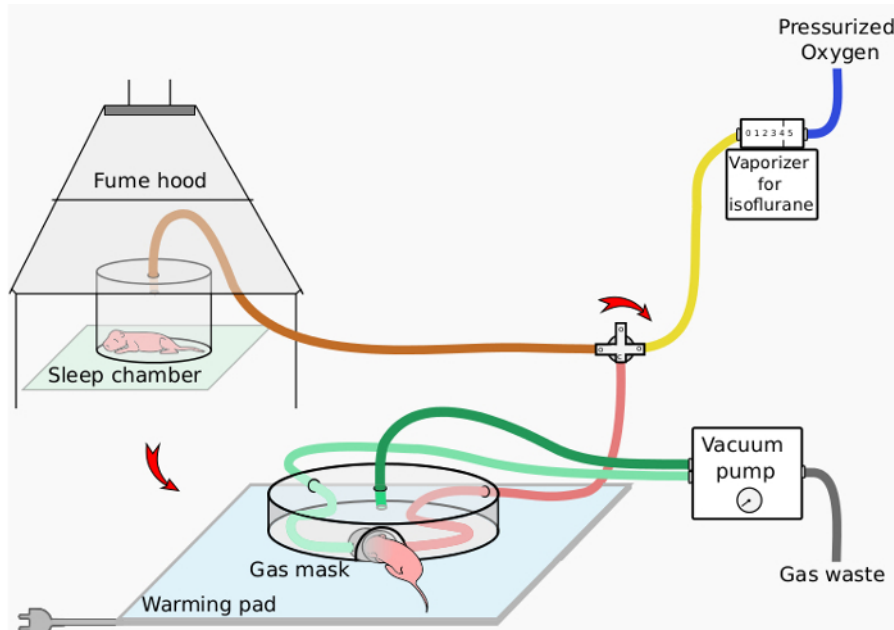


**Figure 1. Schematic of anesthesia setup.** This schematic presents the anesthesia setup designed for the neonatal mouse, with a sleep chamber for initial anesthesia and a nose mask device for continued anesthesia during surgery.

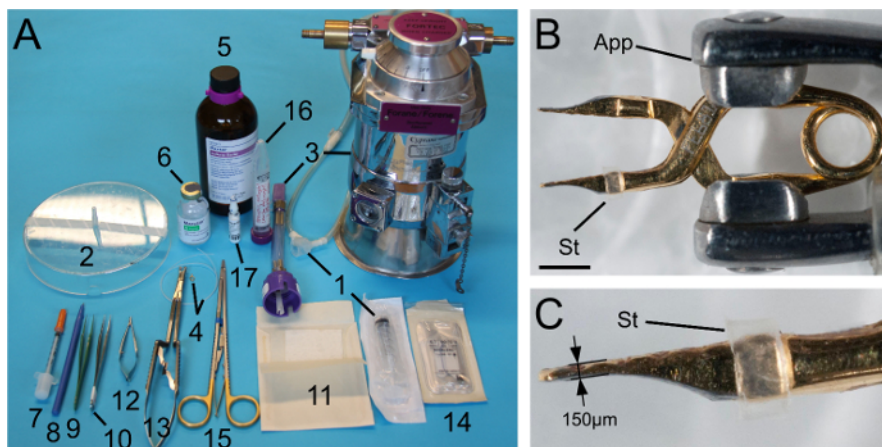


**Figure 2. Principal tools and compression clip.** (A) Tools used during the procedure. The numbers correspond to the annotation used in Table 1. (B and C) A Yasargil temporary aneurysm mini-clip with the tip of each blade manually trimmed down to about 150  $\mu$ m thickness. A stopper made of a slice of polyethylene tubing (Table 1) is placed on one of the blades to prevent full closure of the clip. Scale bar: 2 mm. App: clip applicator (#12 in A); St: stopper. [Please click here to view a larger version of this figure.](#)

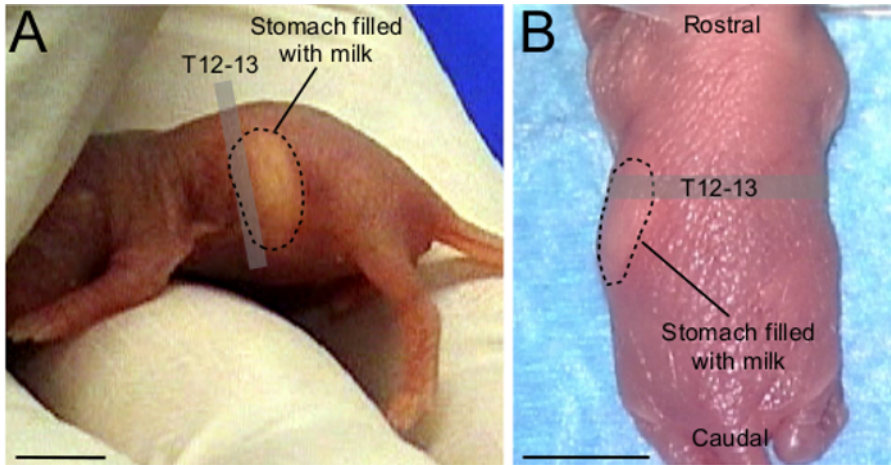


**Figure 3. Landmark for preoperative assessment of spinal level in neonatal ICR mouse.** (A) Lateral view of a P1 ICR mouse with white milk in the stomach. The rostral part of the stomach corresponds to T12-T13 spinal level. (B) P1 ICR mouse under anesthesia in a prone position. Although more difficult to visualize than in (A), the stomach filled with milk is recognizable. The rostral part of the stomach indicates T12-T13 spinal level. Scale bars: 0.5 cm.

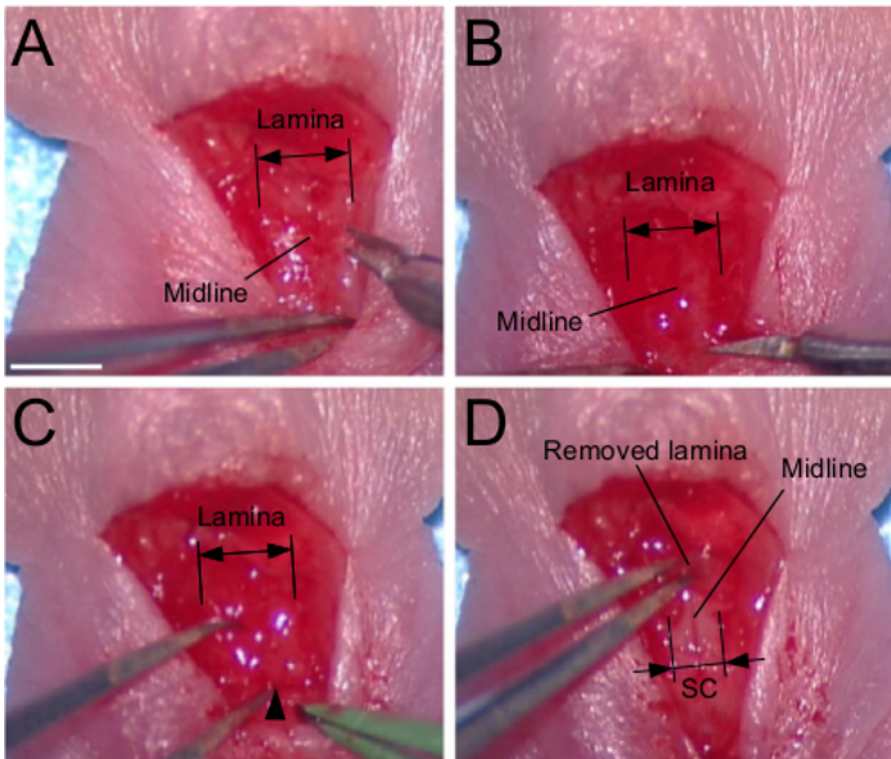


**Figure 4. Dorsal laminectomy.** (A) Dissection of paravertebral muscles. Note that at this age the spinal process is underdeveloped. (B) Transversal sectioning of the lamina with thin scissors. (C) Introduction of one blade of a thin forceps between the lamina and the dura. The entry point is shown by the arrowhead. (D) Removal of the lamina. Scale bar: 2 mm.

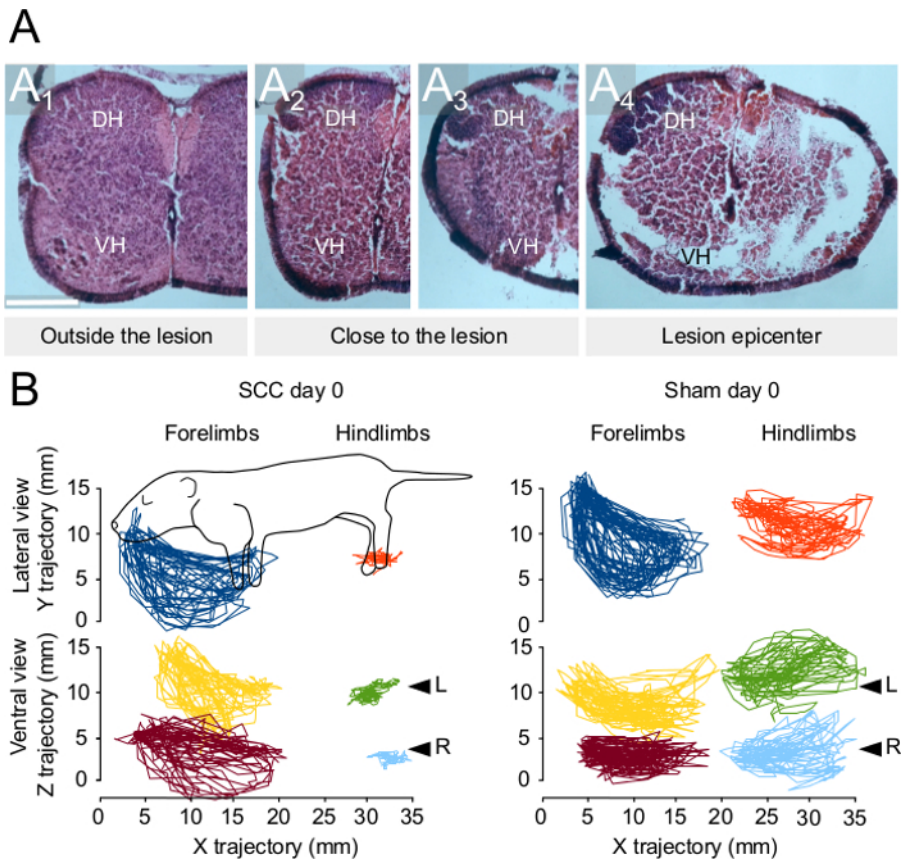


**Figure 5. Histological and behavioral outcomes after spinal cord compression injury at P1.** (A) Eosin and Hematoxylin staining in spinal cord sections from an injured mouse (1 day after injury) at different distance from the injury epicenter. (B) Representative traces of forelimb and hindlimb trajectories observed 6 hours after injury or after a sham control laminectomy. Traces on the top represent trajectories viewed from a lateral view of the animal. Traces at the bottom represent trajectories viewed from the ventral aspect of the animal. See also <sup>1</sup>. Scale bar: 250  $\mu$ m. DH: dorsal horn; L, left; R: right; SCC: spinal cord compression; VH: ventral horn. [Please click here to view a larger version of this figure.](#)

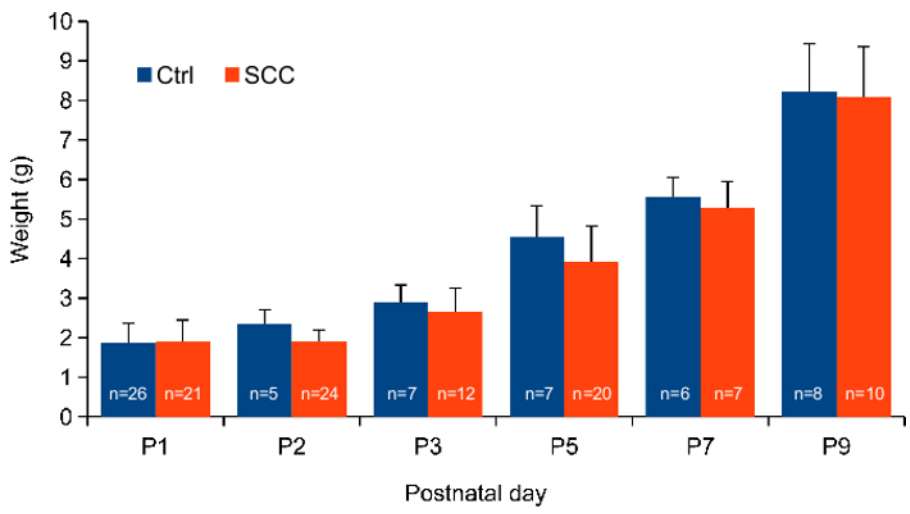


**Figure 6. Comparative growth curves.** Histogram showing the weight gain of unoperated and SCC injured mice from postnatal day 1 to postnatal day 9.

## Discussion

In this article the procedures for a clip-generated SCC injury in P1 mice are described. The same procedures can also be performed at later stages. Compression injuries were performed successfully at P5, P7, P9 and P12 (Züchner, *et al.*, manuscript in preparation). At all postnatal stages, general anesthesia is obtained with isoflurane vaporized in pure oxygen, but the anesthetic outcome depends greatly on age. In initial attempts at P1-P4, before local anesthesia was introduced into the protocol, it was difficult to obtain a deep and prolonged sedation due to a narrow dose-effect window between insufficient sedation and overdose. In addition, concerns related to a neurotoxic effect of isoflurane in

newborn animals have been raised<sup>27-30</sup>. A combination of isoflurane and the local anesthetic Bupivacaine results in a deeper and more stable anesthesia while permitting an isoflurane dose reduction by a factor of 2-3. Different types of anesthesia have been described for neonatal rodents, including cryoanesthesia<sup>31,32</sup>, but one potential inconvenience of cryoanesthesia is its neuroprotective effect (reviewed by<sup>33,34</sup>), which could complicate the generation of an efficient and reproducible injury. Barbiturate-based anesthesia is considered to have lower efficiency in neonatal mice due to lower levels of serum albumin and body fat than in adults<sup>35,36</sup>.

Although quite invasive and traumatic, once the procedure is established the mortality rate during surgery is low. However, there are critical steps during the procedure that require particular attention to improve the recovery and survival of the operated mice. One important issue is to select pups that will have the best chance to survive the surgery. When the litter is large the nutritional state of the individual pups varies. In addition to the unavoidable bleeding that occurs during surgery, operated pups spend hours away from the mother, and they often do not drink milk before the next morning. It is thus an advantage to select pups that already have a certain amount of milk in the stomach. This is readily visible through the abdominal skin from P0 to P7.

During the first night the operated pup is at great risk of being cannibalized by the mother. During initial development of this model more than half of the operated mice were missing the following morning, with clear signs of blood in the cage. Necrophagy, cannibalism and infanticide in rodents have been studied for decades<sup>37-40</sup>. In this study, cannibalism was only witnessed once, but was considered a more likely explanation than necrophagy because the pups that were returned to the cage were typically in such good shape that death by natural causes during the night seemed improbable. This prompted the idea of using a reversible pharmacological agent such as Diazepam to reduce anxiety and aggressiveness in the mother (reviewed by<sup>41</sup>). Intraperitoneal injection of Diazepam greatly improved the situation, dropping mortality during the first night from more than 60% to less than 20%.

Reducing litter size by culling and disturbing the litter as little as possible following postoperative return are additional elements that can benefit the operated animals. However, leaving only operated pups with the mother is not beneficial. The best balance of operated/unoperated pups may vary according to the line, but for ICR and SCID-ICR mice leaving 4-5 operated pups (injury or sham) together with 3-4 unoperated pups gave the best results.

In a general sense, the main limitation of this neonatal SCI model is that the neonatal spinal cord differs in many respects from the adult spinal cord, and thus may not provide experimental results that are comparable to those obtained from adult SCI models. Such differences include overall size and volume of the spinal cord, cell number, under-representation of specific cell types such as oligodendrocytes, immature immune responses and immature neuronal circuits. Conclusions drawn from experiments in this model must therefore be considered carefully. On the other hand, the model is relevant for the relatively less investigated scenario of pediatric SCI. Moreover, the apparent weakness with respect to adult SCI models is also a potential strength as it may allow the elucidation of plasticity mechanisms that, though minimally extant in the adult spinal cord, could represent a therapeutic substrate if reinstated. It is conceivable that reinstatement of neonatal or even embryonic conditions could be implemented through the implantation of less developed cells or tissue or by treatment with reagents that engender the adult tissue with earlier developmental characteristics. Using enzymes to eliminate perineuronal nets is an example of the latter approach<sup>42,43</sup>.

A major issue when establishing an animal model for SCI is to obtain a standardized injury. This is an important aspect that has been addressed in multiple SCI models, e.g., transection, hemisection, impactors, balloon compression, forceps crush, static weight compression, etc. With respect to impacting devices, efforts in this direction have resulted in SCI models in adult rodents where multiple parameters of the impact such as speed, force and duration can be manipulated (reviewed by<sup>44</sup>). Another approach, involving less equipment, employs a modification of the Kerr-Lougheed aneurysm clip<sup>45,46</sup>. These 2 approaches are complementary as the impactor mimics a contusion injury whereas the clip mimics a compression injury with some degree of concurrent ischemia. Because of the substantial size constraints and greater vulnerability of neonatal mice, the higher mortality associated with longer surgeries as well as the costs of developing smaller scale equipment, it was chosen to develop a clip-generated compression rather than an impactor-generated contusion approach. This was accomplished by adapting a commercially available aneurysm mini-clip to accommodate the size of the vertebral column of neonatal mice<sup>1</sup>. Adding a stopper ensures a standardized compression width, and as long as the tension of the clip compresses to the limit of the stopper, the force of the compression during the static phase at minimal width should vary little. What is not standardized is the velocity of the compression during its dynamic phase, since this will vary as the clip tension changes over its lifetime. As the static phase of the compression lasts much longer than the dynamic phase, and there is little to suggest that the spinal cord tissue exerts much of a counterforce against the mini-clip blades, it is likely that the severity of injury is most dependent on the static phase. This, however, remains to be tested. Injury severity is likely to depend on multiple factors, including the static compression force and duration, the velocity of compression and decompression, the position of the mini-clip, and the number of compressions performed at the same site. Thus, combinatorial variation in these parameters could result in the generation of a spectrum of injury severities from weak to severe. Despite the potential for variability, in our previously published study<sup>1</sup> we obtained consistent results at histological, physiological and behavioral levels, so there is little to suggest that acceptable standardization is hard to achieve. We note that in that study we used multiple methods of validation at each level, including behavioral tests such as air-stepping as shown in **Figure 5**.

In this neonatal SCI model the injury spares a certain proportion of axons and thereby provides a situation favorable for eliciting adaptive plasticity through the re-modeling of spared connections and the formation of new circuits. Moreover, since the neonatal mouse is well suited for investigation by many experimental methods, it is possible to use this model to study functional recovery and adaptive plasticity with an integrative approach, including behavioral tests, retrograde and anterograde axonal tracing, immunohistochemistry, electrophysiology and high-throughput optical recording<sup>1</sup>. As an example, we took advantage of this integrative approach to demonstrate network re-modeling at the level of specific descending inputs using high-throughput calcium imaging in *ex vivo* wholemount preparations of the brain stem and injured spinal cord<sup>1</sup>. This can be pushed further by using neuro-optogenetic and optogenetic pharmacology tools to assess the remodeling of synaptic connections among specific subpopulations of spinal neurons.

## Disclosures

The authors have nothing to disclose.

## Acknowledgements

This work has been supported by grants from the South-Eastern Norway Regional Health Authority (JLB, 2014119; JCG, project numbers 2015045 and 2012065), by the Norwegian Research Council (JCG, project number 23 00 00) and the University of Oslo.

## References

- Boulland, J.-L., Lambert, F. M., Züchner, M., Strom, S., & Glover, J. C. A Neonatal Mouse Spinal Cord Injury Model for Assessing Post-Injury Adaptive Plasticity and Human Stem Cell Integration. *PLoS ONE*. **8** (8) (2013).
- Raineteau, O., & Schwab, M. E. Plasticity of motor systems after incomplete spinal cord injury. *Nat. Rev. Neurosci.* **2** (4), 263-273 (2001).
- Edgerton, V. R., Tillakaratne, N. J. K., Bigbee, A. J., de Leon, R. D., & Roy, R. R. Plasticity of the spinal neural circuitry after injury. *Annu. Rev. Neurosci.* **27**, 145-167 (2004).
- Bareyre, F. M., *et al.* The injured spinal cord spontaneously forms a new intraspinal circuit in adult rats. *Nat. Neurosci.* **7** (3), 269-277 (2004).
- Cai, L. L., *et al.* Plasticity of functional connectivity in the adult spinal cord. *Philos. Trans. R. Soc. Lond. B., Biol. Sci.* **361** (1473), 1635-1646 (2006).
- Courtine, G., Song, B., *et al.* Recovery of supraspinal control of stepping via indirect propriospinal relay connections after spinal cord injury. *Nat. Med.* **14** (1), 69-74 (2008).
- Courtine, G., *et al.* Transformation of nonfunctional spinal circuits into functional states after the loss of brain input. *Nat. Neurosci.* **12** (10), 1333-1342 (2009).
- Fenrich, K. K., & Rose, P. K. Axons with highly branched terminal regions successfully regenerate across spinal midline transections in the adult cat. *J. Comp. Neurol.* **519** (16), 3240-3258 (2011).
- Fenrich, K. K., & Rose, P. K. Spinal interneuron axons spontaneously regenerate after spinal cord injury in the adult feline. *J. Neurosci.* **29** (39), 12145-12158 (2009).
- Farrar, M. J., *et al.* Chronic in vivo imaging in the mouse spinal cord using an implanted chamber. *Nat. Methods.* **9** (3), 297-302 (2012).
- Oshima, Y., *et al.* Intravital multiphoton fluorescence imaging and optical manipulation of spinal cord in mice, using a compact fiber laser system. *Lasers Surg. Med.* **46** (7), 563-572 (2014).
- Débarre, D., Olivier, N., Supatto, W., & Beaurepaire, E. Mitigating phototoxicity during multiphoton microscopy of live Drosophila embryos in the 1.0-1.2  $\mu\text{m}$  wavelength range. *PLoS One*. **9** (8), e104250 (2014).
- Kasumacic, N., Glover, J. C., & Perreault, M.-C. Segmental patterns of vestibular-mediated synaptic inputs to axial and limb motoneurons in the neonatal mouse assessed by optical recording. *J. Physiol.* **588** (Pt 24), 4905-4925 (2010).
- Kasumacic, N., Glover, J. C., & Perreault, M.-C. Vestibular-mediated synaptic inputs and pathways to sympathetic preganglionic neurons in the neonatal mouse. *J. Physiol.* **590** (Pt 22), 5809-5826 (2012).
- Szokol, K., Glover, J. C., & Perreault, M.-C. Differential origin of reticulospinal drive to motoneurons innervating trunk and hindlimb muscles in the mouse revealed by optical recording. *J. Physiol.* **586** (Pt 21), 5259-5276 (2008).
- Szokol, K., Glover, J. C., & Perreault, M.-C. Organization of functional synaptic connections between medullary reticulospinal neurons and lumbar descending commissural interneurons in the neonatal mouse. *J. Neurosci.* **31** (12), 4731-4742 (2011).
- Szokol, K., & Perreault, M.-C. Imaging synaptically mediated responses produced by brainstem inputs onto identified spinal neurons in the neonatal mouse. *J. Neurosci. Meth.* **180** (1), 1-8 (2009).
- Pang, D. Spinal cord injury without radiographic abnormality in children, 2 decades later. *Neurosurgery.* **55** (6), 1325-1342; discussion 1342-1343 (2004).
- Lee, J. H., Sung, I. Y., Kang, J. Y., & Park, S. R. Characteristics of pediatric-onset spinal cord injury. *Pediatr. Int.* **51** (2), 254-257 (2009).
- Parent, S., Mac-Thiong, J.-M., Roy-Beaudry, M., Sosa, J. F., & Labelle, H. Spinal cord injury in the pediatric population: a systematic review of the literature. *J. Neurotrauma.* **28** (8), 1515-1524 (2011).
- Basu, S. Spinal injuries in children. *Front Neurol.* **3**, 96 (2012).
- Chien, L.-C., *et al.* Age, sex, and socio-economic status affect the incidence of pediatric spinal cord injury: an eleven-year national cohort study. *PLoS One*. **7** (6), e39264 (2012).
- Maier, I. C., & Schwab, M. E. Sprouting, regeneration and circuit formation in the injured spinal cord: factors and activity. *Philos. T. R. Soc. Lond. B.* **361** (1473), 1611-1634 (2006).
- Schwab, M. E., & Strittmatter, S. M. Nogo limits neural plasticity and recovery from injury. *Curr. Opin. Neurobiol.* **27**, 53-60 (2014).
- Jakeman, L. B., Hoschouer, E. L., & Basso, D. M. Injured mice at the gym: review, results and considerations for combining chondroitinase and locomotor exercise to enhance recovery after spinal cord injury. *Brain Res. Bull.* **84** (4-5), 317-326 (2011).
- Rhodes, K., & Fawcett, J. Chondroitin sulphate proteoglycans: preventing plasticity or protecting the CNS? *J. Anat.* **204** (1), 33-48 (2004).
- Zhu, C., *et al.* Isoflurane anesthesia induced persistent, progressive memory impairment, caused a loss of neural stem cells, and reduced neurogenesis in young, but not adult, rodents. *J. Cereb. Blood Flow Metab.* **30** (5), 1017-1030 (2010).
- Loepke, A. W., *et al.* The effects of neonatal isoflurane exposure in mice on brain cell viability, adult behavior, learning, and memory. *Anesth. Analg.* **108** (1), 90-104 (2009).
- Rothstein, S., Simkins, T., & Nunez, J. L. Response to neonatal anesthesia - effect of sex on anatomical and behavioral outcome. *Neuroscience.* **152** (4), 959-969 (2008).
- Rizzi, S., Carter, L. B., Ori, C., & Jevtovic-Todorovic, V. Clinical Anesthesia Causes Permanent Damage to the Fetal Guinea Pig Brain. *Brain Pathol. (Zurich, Switzerland)*. **18** (2) (2008).
- Janus, C., & Golde, T. The effect of brief neonatal cryoanesthesia on physical development and adult cognitive function in mice. *Behav. Brain Res.* **259**, 253-260 (2014).
- Núñez, J. L., Koss, W. A., & Juraska, J. M. Hippocampal anatomy and water maze performance are affected by neonatal cryoanesthesia in rats of both sexes. *Horm. Behav.* **37** (3), 169-178 (2000).
- Batchelor, P. E., *et al.* Systematic review and meta-analysis of therapeutic hypothermia in animal models of spinal cord injury. *PLoS one*. **8** (8), e71317 (2013).
- Kwon, B. K., *et al.* Hypothermia for spinal cord injury. *The Spine Journal.* **8** (6), 859-874 (2008).

35. Benjamin, M. M. *Outline of veterinary clinical pathology*. (3rd edition), 351pp. (1978).
36. Cunningham, M. G., & McKay, R. D. G. A hypothermic miniaturized stereotaxic instrument for surgery in newborn rats. *J. Neurosci. Methods*. **47** (1-2), 105-114 (1993).
37. Lane-Petter, W. Cannibalism in rats and mice. *Proc. R. Soc. Med.* **61** (12), 1295-1296 (1968).
38. Gandelman, R., & Simon, N. G. Spontaneous pup-killing by mice in response to large litters. *Dev. Psychobiol.* **11** (3), 235-241 (1978).
39. Taylor, G. T. Urinary odors and size protect juvenile laboratory mice from adult male attack. *Dev. Psychobiol.* **15** (2), 171-186 (1982).
40. Weber, E. M., Algers, B., Hultgren, J., & Olsson, I. A. Pup mortality in laboratory mice -- infanticide or not? *Acta Vet. Scand.* **55** (1), 83 (2013).
41. Crawley, J. N. Exploratory behavior models of anxiety in mice. *Neurosci. Biobehav. Rev.* **9** (1), 37-44 (1985).
42. Kwok, J. C. F., Heller, J. P., Zhao, R.-R., & Fawcett, J. W. Targeting inhibitory chondroitin sulphate proteoglycans to promote plasticity after injury. *Methods Mol. Biol. (Clifton, N.J.)*. **1162**, 127-138 (2014).
43. Kwok, J. C. F., Afshari, F., Garcia-Alias, G., & Fawcett, J. W. Proteoglycans in the central nervous system: plasticity, regeneration and their stimulation with chondroitinase ABC. *Restor. Neurol. Neurosci.* **26** (2-3), 131-145 (2008).
44. Young, W. Spinal cord contusion models. *Prog. Brain Res.* **137**, 231-255 (2002).
45. Rivlin, A. S., & Tator, C. H. Regional spinal cord blood flow in rats after severe cord trauma. *J. Neurosurg.* **49** (6), 844-853 (1978).
46. Rivlin, A. S., & Tator, C. H. Effect of duration of acute spinal cord compression in a new acute cord injury model in the rat. *Surg. Neurol.* **10** (1), 38-43 (1978).
47. Joshi, M., & Fehlings, M. G. Development and characterization of a novel, graded model of clip compressive spinal cord injury in the mouse: Part 1. Clip design, behavioral outcomes, and histopathology. *J. Neurotrauma.* **19** (2), 175-190 (2002).
48. Joshi, M., & Fehlings, M. G. Development and characterization of a novel, graded model of clip compressive spinal cord injury in the mouse: Part 2. Quantitative neuroanatomical assessment and analysis of the relationships between axonal tracts, residual tissue, and locomotor recovery. *J. Neurotrauma.* **19** (2), 191-203 (2002).